Inclusive Charmonium Production via Double $c\bar{c}$ in e^+e^- Annihilation

Kui-Yong Liu
Department of Physics, Peking University, Beijing 100871, People's Republic of China and Department of Physics, Liaoning University, Shenyang 110036, People's Republic of China

Zhi-Guo He
Department of Physics, Peking University, Beijing 100871, People's Republic of China

Kuang-Ta Chao
China Center of Advanced Science and Technology (World Laboratory), Beijing 100080, People's Republic of China and Department of Physics, Peking University, Beijing 100871, People's Republic of China

arXiv:hep-ph/0301218v2 29 Jan 2004

Abstract

Motivated by the recent observation of double charm quark pair production by the Belle Collaboration, we calculate the complete $\mathcal{O}(\alpha_s^2)$ inclusive production cross sections for η_c, J/ψ, and χ_{cJ}(J=0, 1, 2) plus $c\bar{c}$ in e^+e^- annihilation through a virtual photon. We consider both color-singlet and color-octet contributions, and give the analytical expressions for these cross sections. The complete color-singlet calculations are compared with the approximate fragmentation calculations as functions of the center-of-mass energy $\sqrt{s}$. We find that most of the fragmentation results substantially overestimate the cross sections (e.g. by a factor of $\sim$4 for χ_{c1} and χ_{c2}) at the Belle and BaBar energy $\sqrt{s} = 10.6$GeV. The fragmentation results become a good approximation only when $\sqrt{s}$ is higher than about 100GeV. We further calculate the color-octet contributions to these cross sections with analytical expressions. We find that while the color-octet contribution to J/ψ inclusive production via double charm is negligible (only about 3%), the color-octet contributions to χ_{c1} and χ_{c2} can be significant.

PACS number(s): 12.40.Nn, 13.85.Ni, 14.40.Gx

1 Introduction

Charnonium is one of the simplest quark-antiquark composite particles. Charmonium physics has played an important role in the study of Quantum Chromodynamics (QCD) both perturbatively and nonperturbatively, since the first charmonium state J/ψ was discovered in 1974. During the past decade, the study of charmonium has become more interesting because of the large difference between the predictions of the color-singlet model and the observations of J/ψ and ψ' production at several experimental facilities e.g. at the Fermilab Tevatron [1].

The newly developed nonrelativistic QCD (NRQCD) factorization formalism [2] allows the infrared safe calculation of inclusive heavy quarkonium production and decay rates. In the NRQCD production mechanism, a heavy quark-antiquark pair can be produced at short distances in a conventional color-singlet or a color-octet state, and then evolves into an observed quarkonium nonperturbatively. With this color-octet mechanism, one may explain the Tevatron data on the surplus production of J/ψ and ψ' at large p_T, though puzzles about their polarizations still remain (for a recent review see [3] and references therein).

To further test the color octet mechanism, it is interesting to study the charmonium production in e^+e^- annihilation. The J/ψ inclusive production in e^+e^- annihilation has been investigated within the color-singlet model [4, 5, 6] and the color-octet model [7, 8, 9]. The angular distribution and energy distribution of color-singlet J/ψ production at $\sqrt{s} =$ 10.6 GeV have been discussed in [6]. In [7] it is found that a clean signature of the color-octet mechanism may be observed in the angular distribution of J/ψ production near the end point region. In [8] contributions of various color-octet as well as color-singlet channels to the J/ψ production cross sections are calculated in a wide range of e^+e^- collider energies. Moreover, the J/ψ polarizations are predicted in [9]. Recently, BaBar [11] and Belle [12] have measured the direct J/ψ production in continuum e^+e^- annihilations at $\sqrt{s} = 10.6$ GeV. The total cross section and the angular distribution seem to favor the NRQCD calculation over the color-singlet model [11], but some issues (e.g. about the momentum distribution and polarization of J/ψ) still remain.

The situation has become even more complicated due to the very recent observation for the double $c\bar{c}$ production associated with J/ψ by Belle[13]. The measured exclusive cross section for $e^+ + e^- \to J/\psi + \eta_c$ process is an order of magnitude larger than the theoretical value[14], and the measured inclusive cross section for $e^+ + e^- \to J/\psi + c\bar{c}$ ($\sim$0.9 pb)[12, 13] is more than five times larger than NRQCD predictions which are only about 0.1-0.2 pb[6, 8, 9, 10] taking into account the differences in the values of the input parameters or methods. Among other attempts to solve the $J/\psi c\bar{c}$ inclusive production problem[15, 16], e^+e^- annihilation into two photons was also studied[17, 18], but the two photon contribution turned to be negligible at $\sqrt{s} = 10.6$GeV, though it could prevail over one photon contribution at higher energies (say, $\sqrt{s} > 20$GeV)[17].

The double $c\bar{c}$ production associated with J/ψ (both exclusively and inclusively) is very puzzling and needs a better understanding for both perturbative and nonperturbative QCD. On the other hand, experimentally, it is not clear whether the copious (even dominant) double $c\bar{c}$ production will also happen for charmonium states other than J/ψ, such as η_c and χ_{cJ}(J=0, 1, 2). Among them the χ_{c1} and χ_{c2} are more interesting since they have large branching fractions decaying into $J/\psi + \gamma$ and might be easier to be detected. In fact, in Ref. [12] the inclusive production for χ_{c1} and χ_{c2} was searched for with the available integrated luminosity of about 30 fb^{-1} at Belle. As more data are collected in the near future at B factories we hope that more accurate measurements for the P-wave and other S-wave charmonium states will be possible. These measurements will be helpful to clarify the problems associated with J/ψ double $c\bar{c}$ production.

On the theoretical side, the calculations for inclusive S-wave and P-wave charmonia production via double $c\bar{c}$ are necessary in the framework of NRQCD, including both the color-singlet and color-octet contributions. When we know the differences between NRQCD predictions and experimental data, we will have to further consider other mechanisms and methods in QCD to explain the differences.

This paper is organized as follows. In Section 2, we will calculate the complete $\mathcal{O}(\alpha_s^2)$ color-singlet inclusive production cross sections for η_c and χ_{cJ}(J=0,1,2) (along with J/ψ) via double $c\bar{c}$ in e^+e^- annihilation through a virtual photon. Then we will compare the complete calculation with the calculation obtained in the charm quark fragmentation limit, and give their ratio as functions of the center-of-mass energies and determine the energy scales at which fragmentation approximations become reliable. In section 3, we will further

estimate the color-octet contributions to J/ψ and χ_{cJ} inclusive cross sections via double charm. Finally, we summarize our results in section 4.

2 Color-singlet contribution to charmonium production via double $c\bar{c}$ in e^+e^- annihilation

The quarkonium can be described in term of Fock states superposition within the NRQCD framework as follows

$$\begin{aligned} \mid \psi_Q > \; &= O(1) \mid Q\bar{Q}[^3S_1^{(1)}] > + O(v) Q\bar{Q}[^3P_J^{(8)}]g > \\ &+ O(v^2) Q\bar{Q}[^1S_0^{(8)}]g > + O(v^2) Q\bar{Q}[^3S_1^{(1,8)}]gg > + \ldots, \end{aligned} \tag{1}$$

$$\begin{aligned} \mid \chi_{cJ} > \; &= O(1) \mid Q\bar{Q}[^3P_J^{(1)}] > + O(v) Q\bar{Q}[^3S_1^{(8)}]g > \\ &+ O(v^2) Q\bar{Q}[^3P_J^{(1,8)}]gg > + \ldots, \end{aligned} \tag{2}$$

where the superscript 1 or 8 labels the color configuration of the Fock Components.

Following the nonrelativistic QCD (NRQCD) factorization formalism, the scattering amplitude of the process $e^-(p_1) + e^+(p_2) \to \gamma^* \to c\bar{c}(^{2S+1}L_J^{(1,8a)})(p) + c(p_c) + \bar{c}(p_{\bar{c}})$ in Fig. 1 and Fig. 2 is given by

$$\begin{aligned} &\mathcal{A}(e^-(p_1) + e^+(p_2) \to c\bar{c}(^{2S+1}L_J^{(1,8a)})(p) + c(p_c) + \bar{c}(p_{\bar{c}})) = \sqrt{C_L} \sum_{L_z S_z} \sum_{s_1 s_2} \sum_{jk} \\ &\times \quad \langle s_1; s_2 \mid SS_z \rangle \langle LL_z; SS_z \mid JJ_z \rangle \langle 3j; \bar{3}k \mid 1, 8a \rangle \\ &\times \quad \begin{cases} \mathcal{A}(e^-(p_1) + e^+(p_2) \to c_j(\frac{p}{2}; s_1) + \bar{c}_k(\frac{p}{2}; s_2) + c_l(\frac{p_c}{2}; s_3) + \bar{c}_i(\frac{p_{\bar{c}}}{2}; s_4)) & (L = S), \\ \epsilon_\alpha^*(L_Z) \mathcal{A}^\alpha(e^-(p_1) + e^+(p_2) \to c_j(\frac{p}{2}; s_1) + \bar{c}_k(\frac{p}{2}; s_2) + c_l(\frac{p_c}{2}; s_3) + \bar{c}_i(\frac{p_{\bar{c}}}{2}; s_4)) & (L = P). \end{cases} \end{aligned} \tag{3}$$

where $c\bar{c}(^{2S+1}L_J^{(1,8a)})$ is the intermediate $c\bar{c}$ pair produced at short distance, which subsequently evolves into a specific charmonium state at long distance, $\mathcal{A}^\alpha$ is the derivative of the amplitude with respect to the relative momentum between the quark and anti-quark in the bound state. For the case of color-singlet state, the coefficient C_L can be related to the origin of the radial wave function (or its derivative) of the bound state as

$$C_S = \frac{1}{4\pi} \mid R_S(0) \mid^2, \quad C_P = \frac{3}{4\pi} \mid R'_P(0) \mid^2 . \tag{4}$$

The spin projection operator can be defined as[19]

$$P_{SS_z}(p; q) \equiv \sum_{s_1 s_2} \langle s_1; s_2 | SS_z \rangle v(\frac{p}{2} + q; s_1) \bar{u}(\frac{p}{2} - q; s_2). \tag{5}$$

We list the spin projection operators and their derivatives with respect to the relative momentum, which we will use in the calculations, as

$$P_{00}(p, 0) = \frac{1}{2\sqrt{2}} \gamma_5 (\not{p} + 2m_c), \tag{6}$$

$$P_{1S_Z}(p,0) = \frac{1}{2\sqrt{2}} \not\epsilon(S_z)(\not p + 2m_c), \tag{7}$$

$$P^{\alpha}_{1S_z}(p,0) = \frac{1}{4\sqrt{2}m_c}[\gamma^{\alpha} \not\epsilon^*(S_z)(\not p + 2m_c) - (\not p - 2m_c) \not\epsilon(S_z)\gamma^{\alpha}]. \tag{8}$$

For P-wave states we need further relations to reduce the polarizations

$$\begin{aligned}
\sum_{L_Z S_Z} \epsilon^{*\alpha}(L_Z)\epsilon^{*\beta}(S_Z)\langle 1L_Z; 1S_Z \mid J=0J_Z=0\rangle &= \frac{1}{\sqrt{3}}(-g^{\alpha\beta} + \frac{p^{\alpha}p^{\beta}}{M^2}) \\
\sum_{L_Z S_Z} \epsilon^{*\alpha}(L_Z)\epsilon^{*\beta}(S_Z)\langle 1L_Z; 1S_Z \mid J=1J_Z\rangle &= -\frac{i}{\sqrt{2}M}\epsilon^{\alpha\beta\lambda\kappa}p_{\kappa}\epsilon^*_{\lambda}(J_z) \\
\sum_{L_Z S_Z} \epsilon^{*\alpha}(L_Z)\epsilon^{*\beta}(S_Z)\langle 1L_Z; 1S_Z \mid J=1J_Z\rangle &= \epsilon^{*\alpha\beta}(J_Z)
\end{aligned} \tag{9}$$

where M is the mass of the charmonium, which equals to $2m_c$ in the nonrelativistic approximation.

The calculation of cross sections for $e^- + e^+ \to \gamma^* \to$ charmonium $+c\bar{c}$ is straightforward. Using the definition in Ref. [6] we get the differential cross section as follows

$$\frac{d\sigma(e^+ + e^- \to \gamma^* \to \text{charmonium} + c\bar{c})}{dz} = \frac{4C_L\alpha^2\alpha_s^2}{81m_c}(S(z) + \frac{\alpha(z)}{3}). \tag{10}$$

where L=S for S-wave, L=P for P-wave and $z = 2E_{J/\psi}/\sqrt{s}$. The functions $S(z)$ and $\alpha(z)$ for different charmonium states are given in the Appendix.

With Eq. (10) we can evaluate the inclusive cross sections for η_c, J/ψ and χ_{cJ}. The input parameters used in the numerical calculations are[20]

$$m_e = 0, \quad m_c = 1.5 \text{ GeV}, \quad \alpha_s(2m_c) = 0.26, \quad \alpha = 1/137, \tag{11}$$

$$\mid R_S(0) \mid^2 = 0.81 \text{ GeV}^3, \qquad \mid R_P(0)' \mid^2 = 0.075 \text{ GeV}^5. \tag{12}$$

Now we give the numerical results at the Belle and BaBar energy $\sqrt{s} = 10.6$ GeV.

$$\sigma(e^+ + e^- \to \gamma^* \to \eta_c + c\bar{c}) = 58.7 \text{ fb} \tag{13}$$

$$\sigma(e^+ + e^- \to \gamma^* \to J/\psi + c\bar{c}) = 148 \text{ fb} \tag{14}$$

$$\sigma(e^+ + e^- \to \gamma^* \to \chi_{c0} + c\bar{c}) = 48.8 \text{ fb} \tag{15}$$

$$\sigma(e^+ + e^- \to \gamma^* \to \chi_{c1} + c\bar{c}) = 13.5 \text{ fb} \tag{16}$$

$$\sigma(e^+ + e^- \to \gamma^* \to \chi_{c2} + c\bar{c}) = 6.30 \text{ fb} \tag{17}$$

The J/ψ production rate is in agreement with other references[6, 8, 9] after taking into account the differences in the values of the input parameters. In the $z \gg \delta$ limit, where δ is defined as $4m_c/\sqrt{s}$, the approximate fragmentation results will be equivalent to the complete

calculations. This is another check for the validity of the complete calculation. Here the fragmentation cross sections are written as

$$\sigma_{frag}(e^+ + e^- \to \gamma^* \to charmonium + c\bar{c}) = 2\sigma(e^+ + e^- \to c\bar{c}) \int_\delta^1 \mathcal{D}_{c\to charmonium}(z)dz, \tag{18}$$

where $\mathcal{D}(z)$ are the charm quark fragmentation functions into S-wave[21] or P-wave[22] charmonia.

The cross sections obtained in the complete calculation and in the fragmentation approximation as functions of the center-of-mass energies are plotted in Fig. 3-7. All these cross sections are in units of $\sigma_{cc} = \sigma(e^+ + e^- \to \gamma^* \to c\bar{c})$, the cross section for e^+e^- annihilating into the $c\bar{c}$ quark pair, times 10^{-4}. One can find that the cross sections in complete calculations and fragmentation approximations (all in units of the cross section for e^+e^- annihilating to the $c\bar{c}$ pair) are proportional to the fragmentation probabilities for the charm quark fragmentating into charmonia when the $\delta \ll 1$ limit is valid. This is just what the fragmentation approach describes. The results in these figures show that except for χ_{c0}, the differences between fragmentation results and complete calculations are large at low energies. At the Belle and BaBar energy $\sqrt{s}$=10.6GeV, the ratios of complete calculations to fragmentation calculations are

$$\frac{\sigma(e^+ + e^- \to \gamma^* \to charmonium + c\bar{c})}{\sigma_{frag}(e^+ + e^- \to \gamma^* \to charmonium + c\bar{c})} = 0.28, 0.58, 0.25, 0.25 \tag{19}$$

for η_c, J/ψ, χ_{c1}, and χ_{c2} respectively. As the center-of-mass energy increases, the ratios of complete calculations to fragmentation results increase and can reach to 90% when the center-of-mass energy is over 100 GeV. Moreover, the cross sections are rather sensitive to the input parameters. If we choose $\alpha = 1/134, \alpha_s = 0.28$, and $\mathrm{m_c} = 1.48$GeV at $\sqrt{s} = 10.6$GeV, the cross sections for $\eta_c, J/\psi$, and χ_{cJ} (J=0,1,2) become 77.0fb, 192fb, 64.2fb, 18.3fb, 8.48fb respectively.

3 Color-octet contribution to J/ψ and χ_{cJ} production via double $c\bar{c}$ in e^+e^- annihilation

We next estimate the color-octet contribution to J/ψ and χ_{cJ} production via double $c\bar{c}$ in e^+e^- annihilation. The Feynman diagrams are showed in Fig 1 and Fig 2.

In Fig. 1, the charmonium comes from the color-octet mediate states $c\bar{c}(^{2S+1}L_J^{(8)})$ by emitting soft gluons at long distances. Here the color-octet contribution can be obtained from the corresponding color-singlet contribution divided by a factor of $\frac{32<\mathcal{O}_1^H(^{2S+1}L_J)>}{3<\mathcal{O}_8^H(^{2S+1}L_J)>}$. The matrix elements $< \mathcal{O}_n^H(^{2S+1}L_J) >$ can be extracted from the Tevatron data for J/ψ and χ_{cJ} production (see Ref. [24] for detailed discussions). Accordingly, with some unavoidable uncertainties we set them as

$$< \mathcal{O}_1^\psi(^3S_1) >= 1.16 \text{ GeV}^3, \tag{20}$$

$$< \mathcal{O}_1^{\chi_{c1}}(^3P_1) >= 0.32 \text{ GeV}^5, \tag{21}$$

$$< \mathcal{O}_8^{\psi}(^3S_1) >= 1.06 \times 10^{-2} \text{ GeV}^3, \tag{22}$$

$$< \mathcal{O}_8^{\psi}(^3P_0) > /m_c^2 = 1.0 \times 10^{-2} \text{ GeV}^3, \tag{23}$$

$$< \mathcal{O}_8^H(^3P_J) >= (2J+1) < \mathcal{O}_8^H(^3P_0) >, \tag{24}$$

$$< \mathcal{O}_8^{\chi_{c1}}(^3S_1) >= 1.0 \times 10^{-2} \text{ GeV}^3. \tag{25}$$

With these values of the matrix elements, the color-octet contributions to J/ψ and χ_{cJ} in Fig. 1 are about at least two orders of magnitude smaller than the color-singlet contributions, and therefore are negligible. In Fig. 2 the color-octet contributions come from four different (the upper two and the lower two) diagrams. With their contributions (including the interference terms), the differential cross section reads

$$\frac{d\sigma_{octet}}{dz} = \frac{16\alpha^2\alpha_s^2 < \mathcal{O}_8^H(^3S_1) >}{27m_c} \mid \bar{M} \mid^2, \tag{26}$$

where $\mid \bar{M} \mid^2$ takes the form

$$\begin{aligned} \mid \bar{M} \mid^2 \;=\; & \frac{\pi}{12\delta^2 s^2 z(z-2)^2}\{-4z\sqrt{\frac{(1-z)(z^2-\delta^2)}{4+\delta^2-4z}} \\ & [3\delta^4 - 12\delta^2(z-2) + 16(10+z(z-10))] + \\ & (z-2)^2[3\delta^4 - 8\delta^2(3z-4) + 32(2+z(z-2))] \\ & \ln[\frac{z\sqrt{4+\delta^2-4z} + 2\sqrt{(1-z)(z^2-\delta^2)}}{z\sqrt{4+\delta^2-4z} - 2\sqrt{(1-z)(z^2-\delta^2)}}]\}. \end{aligned} \tag{27}$$

The numerical results can be obtained by using the parameters given above, and are

$$\sigma_{octet}(e^+e^- \to J/\psi c\bar{c}) = 4.5 \text{ fb}. \tag{28}$$

$$\sigma_{octet}(e^+e^- \to \chi_{c1} c\bar{c}) = 4.3 \text{ fb}. \tag{29}$$

The color-octet contribution to J/ψ is only 3% of the color-singlet cross section. For χ_{c1}, the color-octet contribution is significant, which is about 32% of the color-singlet cross section. With the approximation of heavy quark spin symmetry, the contributions of color octet $^3S_1$ to χ_{cJ} (from color-octet $^3S_1$ mediate state to color-singlet ^3P_J final state by E1 transition) satisfy the ratio $1:3:5$ for $J=0,1,2$ respectively. Their values are given by

$$\sigma_{octet}(e^+e^- \to \chi_{c0} c\bar{c}) = 1.4 \text{ fb}. \tag{30}$$

$$\sigma_{octet}(e^+e^- \to \chi_{c2} c\bar{c}) = 7.2 \text{ fb}. \tag{31}$$

We show the angular distribution and energy distribution for χ_{c1} in Fig 8 and Fig 9. One can see that the color-octet contribution enhances the differential cross section significantly in the low energy (small z) region.

4 Conclusion

In summary, we have calculated the complete $\mathcal{O}(\alpha_s^2)$ inclusive production cross sections for η_c, J/ψ, and χ_{cJ}(J=0, 1, 2) plus $c\bar{c}$ in e^+e^- annihilation through a virtual photon. We consider both color-singlet and color-octet contributions, and give the analytical expressions for these cross sections. The complete color-singlet calculations are compared with the approximate fragmentation calculations as functions of the center-of-mass energy $\sqrt{s}$. We find that most of the fragmentation results substantially overestimate the cross sections (e.g. by a factor of $\sim$4 for χ_{c1} and χ_{c2}) at the Belle and BaBar energy $\sqrt{s} = 10.6$GeV. The fragmentation results become a good approximation only when $\sqrt{s}$ is higher than about 100GeV. We further calculated the color-octet contributions to these cross sections with analytical expressions. We find that while the color-octet contribution to J/ψ inclusive production via double charm is negligible (only about 3%), the color-octet contributions to χ_{c1} and χ_{c2} can be significant. These results may serve as NRQCD predictions to compare with the experimental data observed or to be observed at Belle and BaBar.

Acknowledgments

The authors thank Z.Z. Song for useful discussions. This work was supported in part by the National Natural Science Foundation of China, and the Education Ministry of China.

Appendix

In this Appendix, we give the functions of S and α which are defined in Eq. (10).

$$
\begin{aligned}
\mathrm{S}_{\eta_c} \;=\; & \frac{4\pi}{3s^2\delta^2 z^3(z-2)^6(z^2-\delta^2)}\{4z\sqrt{\frac{(1-z)(z^2-\delta^2)}{4+\delta^2-4z}}[-96\delta^6(2+\delta^2)(4+\delta^2) \\
& +96\delta^6(64+22\delta^2+\delta^4)z-16\delta^2(1920-864\delta^2+532\delta^4+125\delta^6-2\delta^8)z^2 \\
& +8\delta^2(9984-5312\delta^2+488\delta^4+96\delta^6-\delta^8)z^3 \\
& +2(6144-47872\delta^2+20800\delta^4-392\delta^6-110\delta^8+3\delta^{10})z^4 \\
& -4(6144-21376\delta^2+4256\delta^4+112\delta^6+9\delta^8)z^5 \\
& +(14336-51328\delta^2+5472\delta^4+420\delta^6-3\delta^8)z^6 \\
& -4(1536-3168\delta^2+352\delta^4+\delta^6)z^7 \\
& +8(864-36\delta^2+13\delta^4)z^8-32(112+11\delta^2)z^9+768z^{10}] \\
& -3\delta^2(z-2)^4[8\delta^6(2+\delta^2)-96\delta^6 z-2\delta^2(192-48\delta^2+8\delta^4-\delta^6)z^2 \\
& +16\delta^2(8+6\delta^2-\delta^4)z^3+\delta^2(192+40\delta^2-\delta^4)z^4+8(32-4\delta^2+\delta^4)z^5
\end{aligned}
$$

$$-8(48+\delta^2)z^6]\ln\frac{z\sqrt{4+\delta^2-4z}+2\sqrt{(1-z)(z^2-\delta^2)}}{z\sqrt{4+\delta^2-4z}-2\sqrt{(1-z)(z^2-\delta^2)}}\}. \tag{32}$$

$$\begin{aligned}
\alpha_{\eta_c} &= \frac{4\pi}{3s^2\delta^2z^3(z-2)^6(z^2-\delta^2)}\{4z\sqrt{\frac{(1-z)(z^2-\delta^2)}{4+\delta^2-4z}}[96\delta^6(4+\delta^2)(6+\delta^2)\\
&-96\delta^6(64+18\delta^2+\delta^4)z+16\delta^2(2688+608\delta^2+428\delta^4+43\delta^6-2\delta^8)z^2\\
&-8\delta^2(17664+3264\delta^2+184\delta^4-96\delta^6-\delta^8)z^3\\
&+2(6144+89344\delta^2+7744\delta^4-2024\delta^6-174\delta^8-3\delta^{10})z^4\\
&-4(6144+22656\delta^2-1376\delta^4-512\delta^6-35\delta^8)z^5\\
&+(14336+5504\delta^2-5152\delta^4-732\delta^6-3\delta^8)z^6\\
&-4(1536-1760\delta^2-416\delta^4+\delta^6)z^7\\
&+8(864-196\delta^2+13\delta^4)z^8-32(112+11\delta^2)z^9+768z^{10}]\\
&+3\delta^2(z-2)^4[8\delta^6(6+\delta^2)-32\delta^6z-2\delta^2(64+48\delta^2+16\delta^4-\delta^6)z^2\\
&+16\delta^2(12-\delta^2)(2+\delta^2)z^3-(1024+320\delta^2-88\delta^4-\delta^4)z^4\\
&+8(96-28\delta^2-\delta^4)z^5+8(16+\delta^2)z^6]\\
&\times\ln\frac{z\sqrt{4+\delta^2-4z}+2\sqrt{(1-z)(z^2-\delta^2)}}{z\sqrt{4+\delta^2-4z}-2\sqrt{(1-z)(z^2-\delta^2)}}\}.
\end{aligned} \tag{33}$$

$$\begin{aligned}
\mathrm{S}_\psi &= \frac{4\pi}{s^2\delta^2z^3(z-2)^6(z^2-\delta^2)}\{4z\sqrt{\frac{(1-z)(z^2-\delta^2)}{4+\delta^2-4z}}\\
&\times[-32\delta^4(4+\delta^2)(48+22\delta^2+3\delta^4)\\
&+32\delta^4(768+400\delta^2+66\delta^4+3\delta^6)z\\
&-16\delta^2(384+1920\delta^2+556\delta^4+29\delta^6-2\delta^8)z^2\\
&+8\delta^2(1792+128\delta^2-568\delta^4-80\delta^6-\delta^8)z^3\\
&+2(2048-11008\delta^2+10752\delta^4+3176\delta^6+98\delta^8+3\delta^{10})z^4\\
&-4(4096-7808\delta^2+3424\delta^4+600\delta^6+17\delta^8)z^5\\
&+(38912-20608\delta^2+4544\delta^4+508\delta^6-3\delta^8)z^6\\
&-4(13312-800\delta^2+120\delta^4-3\delta^6)z^7+8(4512-20\delta^2-15\delta^4)z^8\\
&-32(336-\delta^2)z^9+1280z^{10}]\\
&-\delta^2(z-2)^4[8\delta^4(48+22\delta^2+3\delta^4)-32\delta^4(24+5\delta^2)z\\
&-2\delta^2(448+16\delta^2+8\delta^4-3\delta^6)z^2+16\delta^2(56-10\delta^2-5\delta^4)z^3\\
&+\delta^2(1152+272\delta^2-3\delta^4)z^4+8(32-92\delta^2+5\delta^4)z^5-56(16+\delta^2)z^6\\
&+512z^7]\ln\frac{z\sqrt{4+\delta^2-4z}+2\sqrt{(1-z)(z^2-\delta^2)}}{z\sqrt{4+\delta^2-4z}-2\sqrt{(1-z)(z^2-\delta^2)}}\}.
\end{aligned} \tag{34}$$

$$\alpha_\psi = \frac{4\pi}{s^2\delta^2z^3(z-2)^6(z^2-\delta^2)}\{4z\sqrt{\frac{(1-z)(z^2-\delta^2)}{4+\delta^2-4z}}$$

$$
\begin{aligned}
&\times[32\delta^4(4+\delta^2)(16+2\delta^2+3\delta^4)-32\delta^4(256+48\delta^2+22\delta^4+3\delta^6)z\\
&+16\delta^2(1152+1024\delta^2-140\delta^4-53\delta^6-2\delta^8)z^2\\
&-8\delta^2(5376+128\delta^2-1576\delta^4-240\delta^6-\delta^8)z^3\\
&+2(2048-768\delta^2-19968\delta^4-6968\delta^6-350\delta^8-3\delta^{10})z^4\\
&-4(4096-20096\delta^2-11168\delta^4-1208\delta^6-43\delta^8)z^5\\
&+(38912-75392\delta^2-16960\delta^4-996\delta^6-3\delta^8)z^6\\
&-4(13312-6304\delta^2-872\delta^4-3\delta^6)z^7+8(4512-500\delta^2-15\delta^4)z^8\\
&-32(336-\delta^2)+1280z^{10}]\\
&+\delta^2(z-2)^4[8\delta^4(16+2\delta^2+3\delta^4)-32\delta^4(8-\delta^2)z\\
&-2\delta^2(320-272\delta^2+64\delta^4-3\delta^6)z^2+16\delta^2(40-54\delta^2-5\delta^4)z^3\\
&-(1024-720\delta^4-3\delta^6)z^4+8(96-36\delta^2-5\delta^4)z^5\\
&+8(80+7\delta^2)z^6-512z^7]\ln\frac{z\sqrt{4+\delta^2-4z}+2\sqrt{(1-z)(z^2-\delta^2)}}{z\sqrt{4+\delta^2-4z}-2\sqrt{(1-z)(z^2-\delta^2)}}\}. \qquad (35)
\end{aligned}
$$

$$
\begin{aligned}
\mathrm{S}_{\chi_{c0}} &= \frac{8\pi}{9s^3\delta^4z^5(z-2)^8(z^2-\delta^2)}\{-4z\sqrt{(1-z)(z^2-\delta^2)(4+\delta^2-4z)}\\
&\times[2304\delta^{10}-1152\delta^8(26+5\delta^2)z+192\delta^6(640+464\delta^2+35\delta^4)z^2\\
&+96\delta^4(1152-4816\delta^2-1136\delta^4-43\delta^6)z^3\\
&+16\delta^2(4608-33024\delta^2+44752\delta^4+4360\delta^6+75\delta^8)z^4\\
&-8\delta^2(21504-123392\delta^2+78448\delta^4+2884\delta^6-45\delta^8)z^5\\
&-4(12288-156672\delta^2+244224\delta^4-78128\delta^6-512\delta^8+21\delta^{10})z^6\\
&-2(24576+549888\delta^2-356096\delta^4+41744\delta^6+80\delta^8-9\delta^{10})z^7\\
&-8(4608-93952\delta^2+45728\delta^4-1206\delta^6+27\delta^8)z^8\\
&+(487424-208384\delta^2+119424\delta^4+696\delta^6-9\delta^8)z^9\\
&-4(155904+4160\delta^2+5216\delta^4-21\delta^6)z^{10}\\
&+16(22976+1480\delta^2+85\delta^4)z^{11}-480(232+11\delta^2)z^{12}+15104z^{13}]\\
&+3\delta^2(z-2)^4[-192\delta^{10}+96\delta^8(26+3\delta^2)z-64\delta^6(160+75\delta^2+3\delta^4)z^2\\
&-16\delta^4(576-1664\delta^2-183\delta^4-2\delta^6)z^3\\
&-4\delta^2(1536-4608\delta^2+4016\delta^4+152\delta^6+5\delta^8)z^4\\
&+2\delta^2(11264-23424\delta^2-160\delta^4+106\delta^6+3\delta^8)z^5\\
&+4(2048-4224\delta^2+9952\delta^4+248\delta^6-27\delta^8)z^6\\
&-(20480-22528\delta^2+5312\delta^4-368\delta^6+3\delta^8)z^7\\
&+4(4096-6496\delta^2-600\delta^4+17\delta^6)z^8-16(320-472\delta^2+7\delta^4)z^9\\
&+32(48+\delta^2)z^{10}]\ln\frac{z\sqrt{4+\delta^2-4z}+2\sqrt{(1-z)(z^2-\delta^2)}}{z\sqrt{4+\delta^2-4z}-2\sqrt{(1-z)(z^2-\delta^2)}}\}. \qquad (36)
\end{aligned}
$$

$$
\alpha_{\chi_{c0}} = \frac{8\pi}{9s^3\delta^4z^5(z-2)^8(z^2-\delta^2)}\{4z\sqrt{(1-z)(z^2-\delta^2)(4+\delta^2-4z)}
$$

$$
\begin{aligned}
&\times[2304\delta^{10}-5760\delta^{8}(6+\delta^{2})z+192\delta^{6}(896+424\delta^{2}+35\delta^{4})z^{2}\\
&+96\delta^{4}(384-4528\delta^{2}-904\delta^{4}-43\delta^{6})z^{3}\\
&+16\delta^{2}(1536+3840\delta^{2}+23536\delta^{4}+2992\delta^{6}+75\delta^{8})z^{4}\\
&-8\delta^{2}(52224+8704\delta^{2}+3280\delta^{4}+1924\delta^{6}-45\delta^{8})z^{5}\\
&+4(12288+70656\delta^{2}-51200\delta^{4}-34224\delta^{6}-232\delta^{8}-21\delta^{10})z^{6}\\
&+2(24576+336896\delta^{2}+133888\delta^{4}+53904\delta^{6}+376\delta^{8}+9\delta^{10})z^{7}\\
&+16(2304-62720\delta^{2}-11280\delta^{4}-2191\delta^{6}-30\delta^{8})z^{8}\\
&-(487424-605696\delta^{2}-61312\delta^{4}-7016\delta^{6}-9\delta^{8})z^{9}\\
&+4(155904-40768\delta^{2}-2560\delta^{4}-21\delta^{6})z^{10}\\
&-16(22976-504\delta^{2}+85\delta^{4})z^{11}+480(232+11\delta^{2})z^{12}-15104z^{13}]\\
&+3\delta^{2}(z-2)^{4}[192\delta^{10}-288\delta^{8}(10+\delta^{2})z+64\delta^{6}(224+59\delta^{2}+3\delta^{4})z^{2}\\
&+16\delta^{4}(192-1248\delta^{2}-121\delta^{4}-2\delta^{6})z^{3}\\
&+4\delta^{2}(512-12288\delta^{2}+2384\delta^{4}-56\delta^{6}+5\delta^{8})z^{4}\\
&+2\delta^{2}(3072+35968\delta^{2}-160\delta^{4}+50\delta^{6}-3\delta^{8})z^{5}\\
&-4(2048-4992\delta^{2}+8224\delta^{4}-408\delta^{6}-23\delta^{8})z^{6}\\
&+(12288-51200\delta^{2}-3008\delta^{4}-1456\delta^{6}-3\delta^{8})z^{7}\\
&-4(2048-8992\delta^{2}-1224\delta^{4}-17\delta^{6})z^{8}+16(192-616\delta^{2}-7\delta^{4})z^{9}\\
&+32(16+\delta^{2})z^{10}]\ln\frac{z\sqrt{4+\delta^{2}-4z}+2\sqrt{(1-z)(z^{2}-\delta^{2})}}{z\sqrt{4+\delta^{2}-4z}-2\sqrt{(1-z)(z^{2}-\delta^{2})}}\}. \qquad (37)
\end{aligned}
$$

$$
\begin{aligned}
\mathrm{S}_{\chi_{c1}} \;=\; &\frac{-8\pi}{3s^{3}\delta^{4}z^{5}(z-2)^{8}(z^{2}-\delta^{2})}\{4z\sqrt{\frac{(1-z)(z^{2}-\delta^{2})}{(4+\delta^{2}-4z)}}[2304\delta^{8}(3+\delta^{2})(4+\delta^{2})\\
&-1152\delta^{6}(192+208\delta^{2}+62\delta^{4}+5\delta^{6})z\\
&+192\delta^{4}(3072+6400\delta^{2}+3568\delta^{4}+668\delta^{6}+35\delta^{8})z^{2}\\
&-96\delta^{4}(26624+27808\delta^{2}+9992\delta^{4}+1276\delta^{6}+43\delta^{8})z^{3}\\
&+16\delta^{2}(36864+277248\delta^{2}+195296\delta^{4}+50464\delta^{6}+4406\delta^{8}+75\delta^{10})z^{4}\\
&-8\delta^{2}(258048+521984\delta^{2}+302624\delta^{4}+57800\delta^{6}+2672\delta^{8}-45\delta^{10})z^{5}\\
&-4(98304-753664\delta^{2}-564992\delta^{4}-310048\delta^{6}-37736\delta^{8}-172\delta^{10}+21\delta^{12})z^{6}\\
&+2(983040-659456\delta^{2}+84480\delta^{4}-103008\delta^{6}-9000\delta^{8}-220\delta^{10}+9\delta^{12})z^{7}\\
&-(4784128+2330624\delta^{2}+1528576\delta^{4}+120800\delta^{6}+396\delta^{8}+117\delta^{10})z^{8}\\
&+(6914048+3928064\delta^{2}+1137792\delta^{4}+74544\delta^{6}+1900\delta^{8}-9\delta^{10})z^{9}\\
&-2(3100672+1294336\delta^{2}+200672\delta^{4}+8036\delta^{6}-9\delta^{8})z^{10}\\
&+8(443392+116992\delta^{2}+8048\delta^{4}+35\delta^{6})z^{11}\\
&-64(20288+2808\delta^{2}+51\delta^{4})z^{12}+512(544+33\delta^{2})z^{13}-28672z^{14}]\\
&-3\delta^{2}(z-2)^{4}[-192\delta^{8}(3+\delta^{2})+96\delta^{6}(48+28\delta^{2}+3\delta^{4})z\\
&-16\delta^{4}(768+808\delta^{2}+217\delta^{4}+12\delta^{6})z^{2}\\
&+16\delta^{4}(1600+652\delta^{2}+105\delta^{4}+2\delta^{6})z^{3}
\end{aligned}
$$

$$
\begin{aligned}
&+4\delta^2(7168-4352\delta^2-360\delta^4-59\delta^6-5\delta^8)z^4\\
&-2\delta^2(24576-3968\delta^2+1024\delta^4-64\delta^6-3\delta^8)z^5\\
&+\delta^2(17408-7296\delta^2+136\delta^4-51\delta^6)z^6\\
&-(8192-12800\delta^2-8576\delta^4-300\delta^6+3\delta^8)z^7\\
&+2(8192-6656\delta^2-1328\delta^4+17\delta^6)z^8-128(80-10\delta^2+\delta^4)z^9\\
&+128(24+5\delta^2)z^{10}]\ln\frac{z\sqrt{4+\delta^2-4z}+2\sqrt{(1-z)(z^2-\delta^2)}}{z\sqrt{4+\delta^2-4z}-2\sqrt{(1-z)(z^2-\delta^2)}}\}. \qquad (38)
\end{aligned}
$$

$$
\begin{aligned}
\alpha_{\chi_{c1}} \;=\;& \frac{-8\pi}{3s^3\delta^4z^5(z-2)^8(z^2-\delta^2)}\{-4z\sqrt{\frac{(1-z)(z^2-\delta^2)}{(4+\delta^2-4z)}}[2304\delta^8(1+\delta^2)(4+\delta^2)\\
&-1152\delta^6(64+80\delta^2+42\delta^4+5\delta^6)z\\
&+192\delta^4(1024+2432\delta^2+1360\delta^4+404\delta^6+35\delta^8)z^2\\
&-96\delta^4(8192+11872\delta^2+3640\delta^4+652\delta^6+43\delta^8)z^3\\
&+16\delta^2(110592+58624\delta^2+71328\delta^4+12864\delta^6+1522\delta^8+75\delta^{10})z^4\\
&-8\delta^2(724992-245504\delta^2-21024\delta^4-72\delta^6+136\delta^8-45\delta^{10})z^5\\
&+4(98304+1392640\delta^2-1900288\delta^4-349344\delta^6-20648\delta^8-1756\delta^{10}-21\delta^{12})z^6\\
&-2(983040-856064\delta^2-5078528\delta^4-704352\delta^6-37736\delta^8-724\delta^{10}-9\delta^{12})z^7\\
&+(4784128-7352320\delta^2-7412992\delta^4-760736\delta^6-20452\delta^8-447\delta^{10})z^8\\
&-(6914048-6197248\delta^2-3225472\delta^4-202576\delta^6-4772\delta^8-9\delta^{10})z^9\\
&+2(3100672-1243136\delta^2-376864\delta^4-15260\delta^6-9\delta^8)z^{10}\\
&-8(443392-47360\delta^2-10128\delta^4+35\delta^6)z^{11}+64(20288+472\delta^2+51\delta^4)z^{12}\\
&-512(544+33\delta^2)z^{13}+28672z^{14}]\\
&+3\delta^2(z-2)^4[-192\delta^8(1+\delta^2)+96\delta^6(16+12\delta^2+3\delta^4)z\\
&-16\delta^4(256+344\delta^2+59\delta^4+12\delta^6)z^2+16\delta^4(448+404\delta^2-9\delta^4+2\delta^6)z^3\\
&+4\delta^2(5120+1792\delta^2-856\delta^4+135\delta^6-5\delta^8)z^4\\
&-2\delta^2(16384+6016\delta^2-1088\delta^4+24\delta^6-3\delta^8)z^5\\
&+(32768-25600\delta^2-7040\delta^4-1864\delta^6-57\delta^8)z^6\\
&-(57344-81408\delta^2-11904\delta^4-884\delta^6-3\delta^8)z^7\\
&+2(16384-27648\delta^2-2384\delta^4-17\delta^6)z^8-128(48-118\delta^2-\delta^4)z^9\\
&-128(8+5\delta^2)z^{10}]\ln\frac{z\sqrt{4+\delta^2-4z}+2\sqrt{(1-z)(z^2-\delta^2)}}{z\sqrt{4+\delta^2-4z}-2\sqrt{(1-z)(z^2-\delta^2)}}\}. \qquad (39)
\end{aligned}
$$

$$
\begin{aligned}
\mathrm{S}_{\chi_{c2}} \;=\;& \frac{-8\pi}{9s^3\delta^4z^5(z-2)^8(z^2-\delta^2)}\{4z\sqrt{\frac{(1-z)(z^2-\delta^2)}{(4+\delta^2-4z)}}\\
&\times[2304\delta^6(4+\delta^2)(144+57\delta^2+5\delta^4)-1152\delta^6(6336+3424\delta^2+558\delta^4+25\delta^6)z\\
&-192\delta^4(12288-82496\delta^2-39168\delta^4-5180\delta^6-175\delta^8)z^2
\end{aligned}
$$

$$
\begin{aligned}
&+96\delta^4(125952-175584\delta^2-80408\delta^4-8852\delta^6-215\delta^8)z^3\\
&+16\delta^2(73728-1579776\delta^2+532640\delta^4+310240\delta^6+29834\delta^8+375\delta^{10})z^4\\
&-8\delta^2(651264-3396352\delta^2+224480\delta^4+323960\delta^6+24824\delta^8-225\delta^{10})z^5\\
&-4(98304-2469888\delta^2+3741440\delta^4-280928\delta^6-327288\delta^8\\
&-15148\delta^{10}+105\delta^{12})z^6+2(1179648-5492736\delta^2\\
&+1172992\delta^4-796064\delta^6-273016\delta^8-9940\delta^{10}+45\delta^{12})z^7\\
&-(7471104-8568832\delta^2-2286336\delta^4-864288\delta^6-131084\delta^8-1377\delta^{10})z^8\\
&+(14909440-4112384\delta^2-1213056\delta^4-33264\delta^6+1164\delta^8-45\delta^{10})z^9\\
&-2(9654272+318976\delta^2+139168\delta^4+39524\delta^6+447\delta^8)z^{10}\\
&+8(1980416+242048\delta^2+25120\delta^4+883\delta^6)z^{11}\\
&-64(119296+10832\delta^2+245\delta^4)z^{12}+1024(1840+73\delta^2)z^{13}-188416z^{14}]\\
&-3\delta^2(z-2)^4[-192\delta^6(144+57\delta^2+5\delta^4)+96\delta^6(1008+304\delta^2+15\delta^4)z\\
&+16\delta^4(4224-6392\delta^2-1731\delta^4-60\delta^6)z^2\\
&-16\delta^4(13632-916\delta^2-705\delta^4-10\delta^6)z^3\\
&-4\delta^2(15360-56448\delta^2-8648\delta^4+433\delta^6+25\delta^8)z^4\\
&+2\delta^2(96256-29568\delta^2-13280\delta^4-340\delta^6+15\delta^8)z^5\\
&+(16384-193536\delta^2-28672\delta^4+14680\delta^6+399\delta^8)z^6\\
&-5(8192-11776\delta^2-3712\delta^4+604\delta^6+3\delta^8)z^7\\
&+2(10240+9728\delta^2-2784\delta^4-79\delta^6)z^8+512(4-47\delta^2+2\delta^4)z^9\\
&+256(12+19\delta^2)z^{10}]\ln\frac{z\sqrt{4+\delta^2-4z}+2\sqrt{(1-z)(z^2-\delta^2)}}{z\sqrt{4+\delta^2-4z}-2\sqrt{(1-z)(z^2-\delta^2)}}\}. \qquad (40)
\end{aligned}
$$

$$
\begin{aligned}
\alpha_{\chi_{c2}} \;=\; &\frac{8\pi}{9s^3\delta^4z^5(z-2)^8(z^2-\delta^2)}\{4z\sqrt{\frac{(1-z)(z^2-\delta^2)}{(4+\delta^2-4z)}}\\
&\times[2304\delta^6(4+\delta^2)(48+3\delta^2+5\delta^4)-1152\delta^6(2112+576\delta^2+170\delta^4+25\delta^6)z\\
&-192\delta^4(6144-33088\delta^2-7296\delta^4-1428\delta^6-175\delta^8)z^2\\
&+96\delta^4(64512-102688\delta^2-16232\delta^4-1860\delta^6-215\delta^8)z^3\\
&-16\delta^2(24576+1006848\delta^2-639968\delta^4-83584\delta^6-5006\delta^8-375\delta^{10})z^4\\
&+8\delta^2(552960+3044608\delta^2-1287968\delta^4-209864\delta^6-6608\delta^8+225\delta^{10})z^5\\
&+4(98304-4091904\delta^2-5157120\delta^4+2831904\delta^6+398216\delta^8\\
&+2884\delta^{10}-105\delta^{12})z^6-2(1179648-15978496\delta^2\\
&-5100032\delta^4+4153696\delta^6+362376\delta^8+4228\delta^{10}-45\delta^{12})z^7\\
&+(7471104-38830080\delta^2-5298944\delta^4+3212896\delta^6+207588\delta^8-285\delta^{10})z^8\\
&-(14909440-29458432\delta^2-3163776\delta^4+769936\delta^6+15836\delta^8-45\delta^{10})z^9\\
&+2(9654272-5982720\delta^2-388704\delta^4+34020\delta^6+447\delta^8)z^{10}\\
&-8(1980416-193664\delta^2-9312\delta^4+883\delta^6)z^{11}\\
&+64(119296+3792\delta^2+245\delta^4)z^{12}-1024(1840+73\delta^2)z^{13}+188416z^{14}]
\end{aligned}
$$

$$
\begin{aligned}
&-3\delta^2(z-2)^4[-192\delta^6(48+3\delta^2+5\delta^4)+288\delta^6(112+8\delta^2+5\delta^4)z \\
&+16\delta^4(1920-3784\delta^2+71\delta^4-60\delta^6)z^2 \\
&-16\delta^4(6336-3660\delta^2+289\delta^4-10\delta^6)z^3 \\
&-4\delta^2(13312-43392\delta^2+9928\delta^4-805\delta^6+25\delta^8)z^4 \\
&+2\delta^2(92160-76928\delta^2+6944\delta^4-676\delta^6+15\delta^8)z^5 \\
&+(16384-322560\delta^2+121856\delta^4+10920\delta^6+365\delta^8)z^6 \\
&-(24576-248320\delta^2+96896\delta^4+5332\delta^6-15\delta^8)z^7 \\
&+2(14336-40960\delta^2+12768\delta^4+79\delta^6)z^8-512(36-55\delta^2+2\delta^4)z^9 \\
&-256(4+19\delta^2)z^{10}]\ln\frac{z\sqrt{4+\delta^2-4z}+2\sqrt{(1-z)(z^2-\delta^2)}}{z\sqrt{4+\delta^2-4z}-2\sqrt{(1-z)(z^2-\delta^2)}}\}. \qquad (41)
\end{aligned}
$$

References

[1] CDF Collaboration, F.Abe *et al.*, Phys. Rev. Lett. **69** 3704 (1992); Phys. Rev. Lett. **71**, 2537 (1993).

[2] G.T. Bodwin, L. Braaten, and G. P. Lepage, Phys. Rev. D51, 1125 (1995).

[3] M. Krämer, Nucl. Phys. **B** (Proc. Suppl.) **93**, 176 (2001).

[4] J.H. Kühn, J. Kaplan, and E.G.O. Sadiani, Nucl. Phys. **B 157**, 125 (1979); W.Y. Keung, Phys. Rev. **D 23**, 2072 (1981); J.H. Kühn and H. Schneider, Phys. Rev. **D 24**, 2996 (1981); J.H. Kühn and H. Schneider, Z. Phys. **C 11**,263 (1981); L. Clavelli, Phys. Rev. **D26**, 1610 (1982).

[5] K. Hagiwara, A.D. Martin and W.J. Stirling, Phys. Lett. **B267**, 527 (1991); V.M. Driesen, J.H. Kühn and E. Mirkes, Phys. Rev.**D 49**, 3197 (1994).

[6] P. Cho and K. Leibovich, Phys. Rev. **D 54**, 6990 (1996).

[7] E. Braaten and Y.-Q. Chen, Phys. Rev. Lett. **76**, 730 (1996).

[8] F. Yuan, C.F. Qiao, and K.T. Chao, Phys. Rev. **D 56**, 321 (1997); *ibid*, 1663 (1997).

[9] S. Baek, P. Ko, J. Lee, and H.S. Song, J. Korean Phys. Soc. **33**, 97 (1998).

[10] V.V. Kiselev *et al.*, Phys. Lett. **B332**, 411 (1994).

[11] BaBar Collaboration, B. Aubert *et al.*, Phys. Rev. Lett. **87**,162002 (2001).

[12] Belle Collaboration, K. Abe *et al.*, Phys. Rev. Lett. **88**, 052001(2002).

[13] Belle Colleboration, K. Abe, *et al.*, Phys. Rev, Lett. **89**, 142001(2002).

[14] E.Braaten and Jungil Lee, Phys. Rev. **D 67**, 054007 (2003); K.Y.Liu, Z.G.He and K.T.Chao, Phys. Lett. **B557**, 45 (2003); K.Hagiwara, E.Kou, and C.F.Qiao, Phys. Lett. **B570**, 39(2003).

[15] B.L.Ioffe and D.E.Kharzeev, hep-ph/0306062.

[16] A.V.Berezhnoy and A.K.Likhoded, hep-ph/0303145.

[17] K.Y.Liu, Z.G.He, and K.T.Chao, Phys. Rev. **D 68**, 031501 (2003) (hep-ph/0305084).

[18] A.V.Luchinsky, hep-ph/0305253.

[19] J.H. Kühn, J. Kaolan and E.G.O. Safiani, Nucl. Phys. **B157**, 125 (1979); B. Guberina, J.H. Kühn, R.D. Peccei and R. Rückl, Nucl. Phys. **B174**, 317(1980);P. Cho and A.K. Leibovich Phys. Rev. **D53**, 150(1996).

[20] E.J. Eichten and C. Quigg, Phys. Rev. **D52**, 1726 (1995).

[21] E.Braaten, K.Cheung and T.C.Yuan, Phys. Rev. **D48**, 4230(1993).

[22] T.C.Yuan, Phys. Rev. **D50**, 5664(1994); J.P.Ma, Phys. Rev. **D53**, 1185(1996).

[23] K.Cheung and T.C.Yuan, Phys. Rev. **D53**, 3591(1995)

[24] P.Cho and A.K.Leibovich, Phys. Rev. **D53**, (1996)6203; P.Cho and A.K.Leibovich, Phys. Rev. **D53**, (1996)150; M.Beneke and M.Krämer, Phys. Rev. **D55**, (1997)5269.

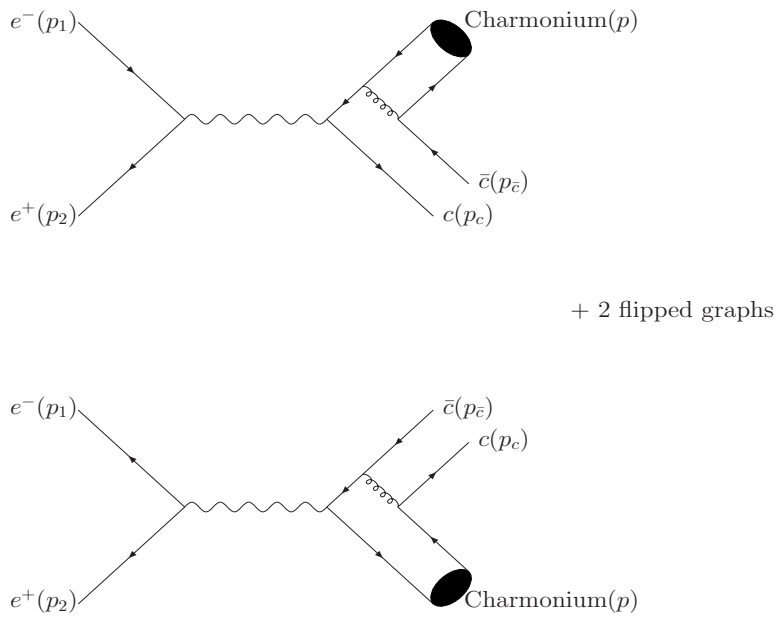

Figure 1: Feynman diagrams for $e^+ + e^- \to \gamma^* \to$ Charmonium $+ c\bar{c}$.

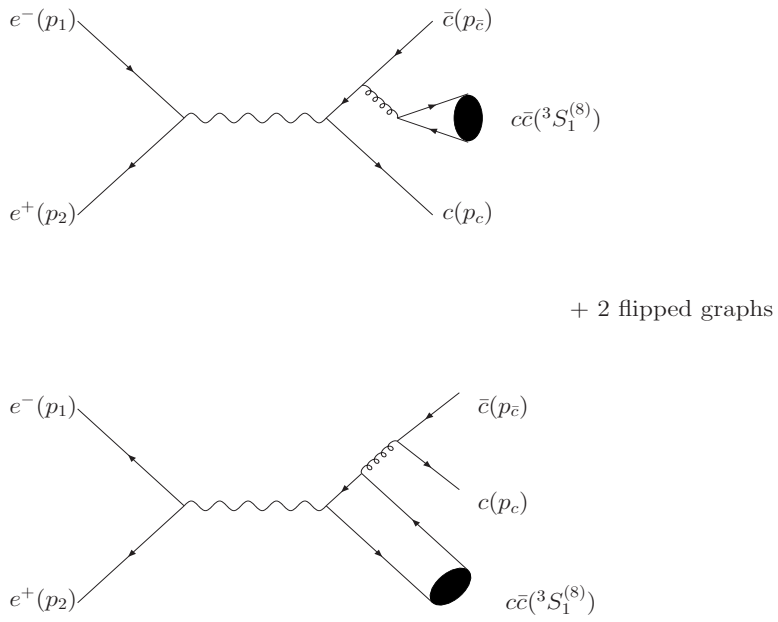

Figure 2: Feynman diagrams for $e^+ + e^- \to \gamma^* \to c\bar{c}(^{2S+1}L_J^{(8)}) + c\bar{c}$.

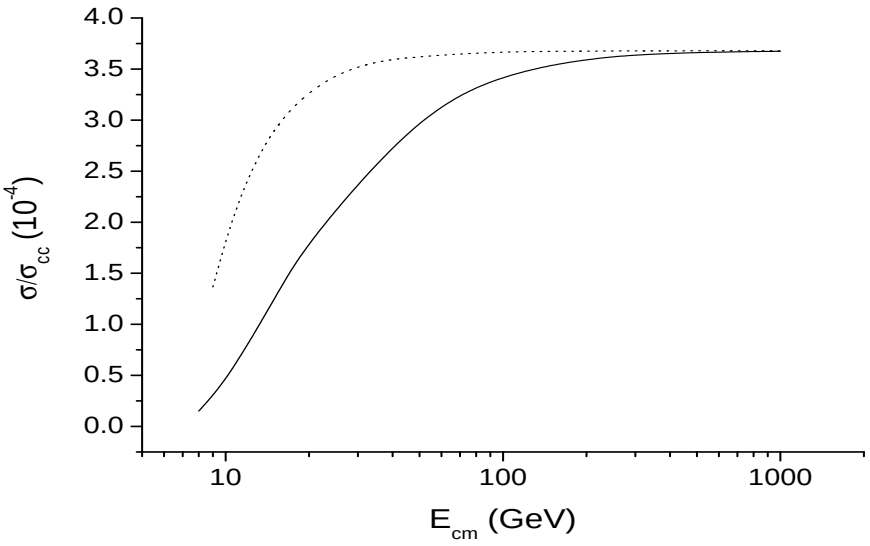

Figure 3: Cross sections for $e^+e^- \to \eta_c + c\bar{c}$ plotted against the center-of-mass energy. Dotted line illustrates the fragmentation calculation and solid line illustrates the complete calculation. The cross sections are in units of $\sigma_{cc} = \sigma(e^+ + e^- \to \gamma^* \to c\bar{c})$ times 10^{-4}.

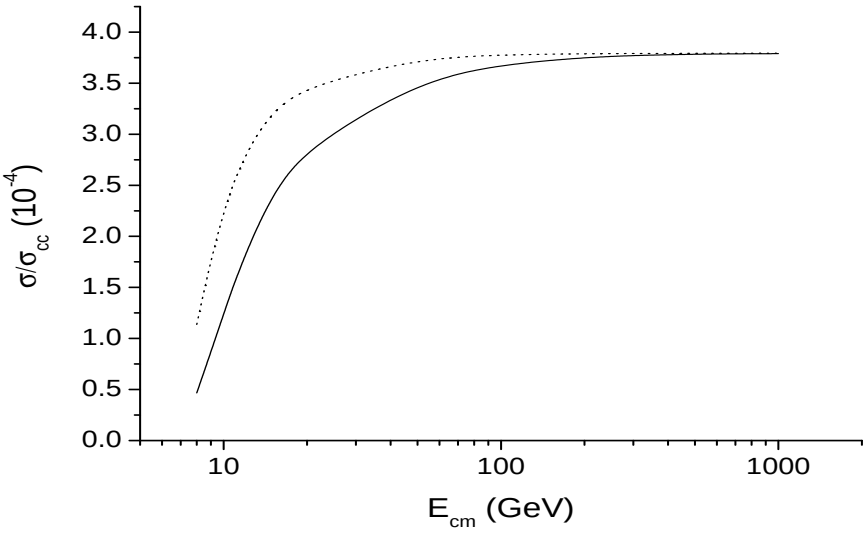

Figure 4: Cross sections for $e^+e^- \to J/\psi + c\bar{c}$ plotted against the center-of-mass energy. Dotted line illustrates the fragmentation calculation and solid line illustrates the complete calculation.

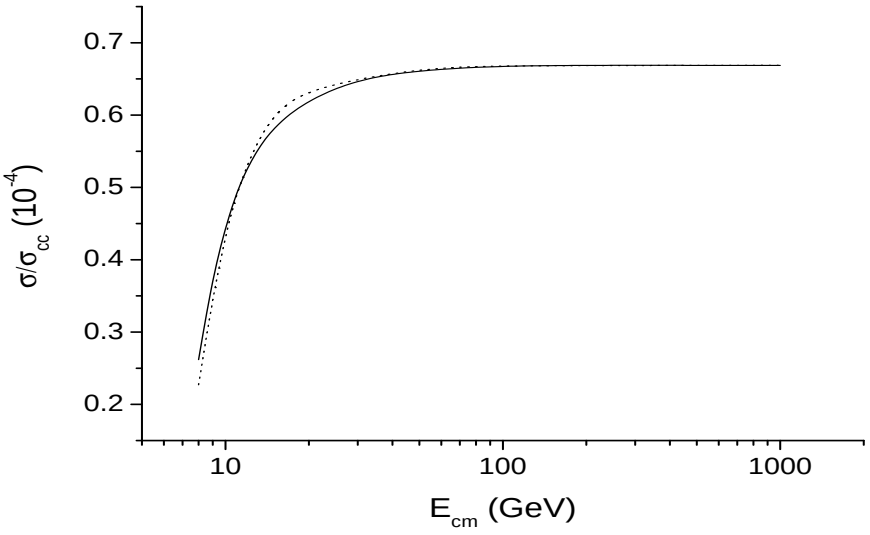

Figure 5: Cross sections for $e^+e^- \to \chi_{c0} + c\bar{c}$ plotted against the center-of-mass energy. Dotted line illustrates the fragmentation calculation and solid line illustrates the complete calculation.

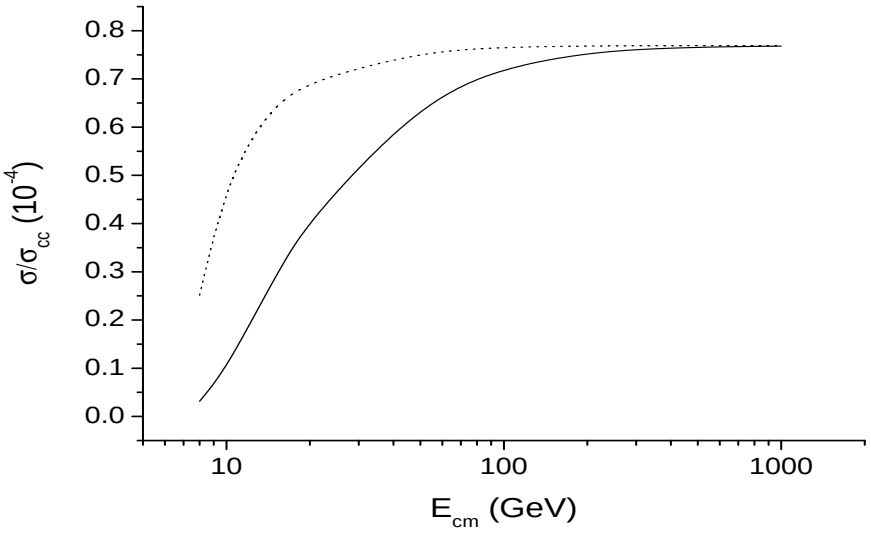

Figure 6: Cross sections for $e^+e^- \to \chi_{c1} + c\bar{c}$ plotted against the center-of-mass energy. Dotted line illustrates the fragmentation calculation and solid line illustrates the complete calculation.

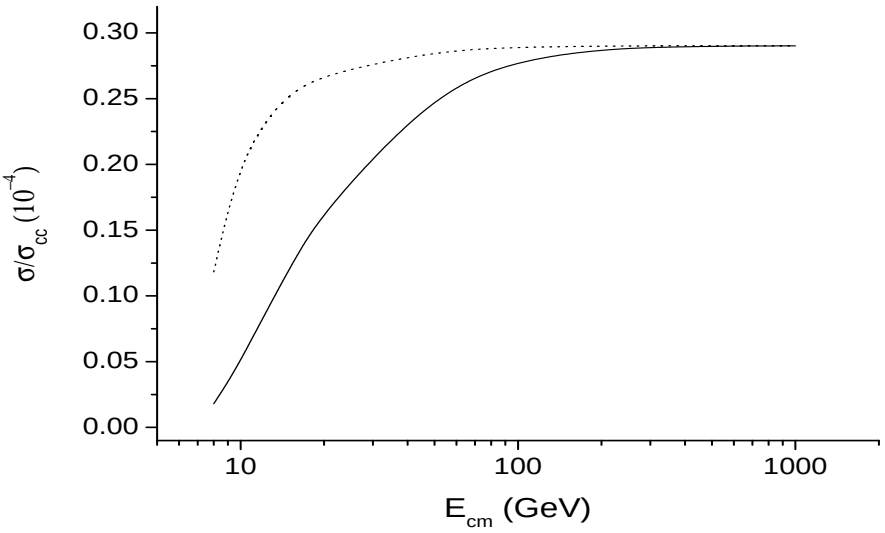

Figure 7: Cross sections for $e^+e^- \to \chi_{c2} + c\bar{c}$ plotted against the center-of-mass energy. Dotted line illustrates the fragmentation calculation and solid line illustrates the complete calculation.

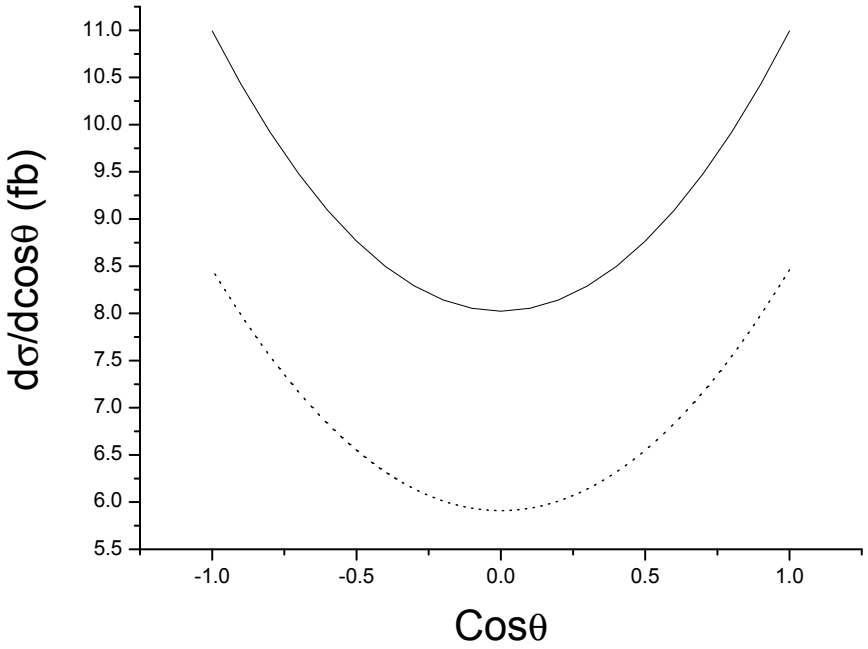

Figure 8: Differential cross sections of the color-singlet (dotted line) and the sum of color-singlet and color-octet (solid line) contributions as functions of the production angle of χ_{c1}.

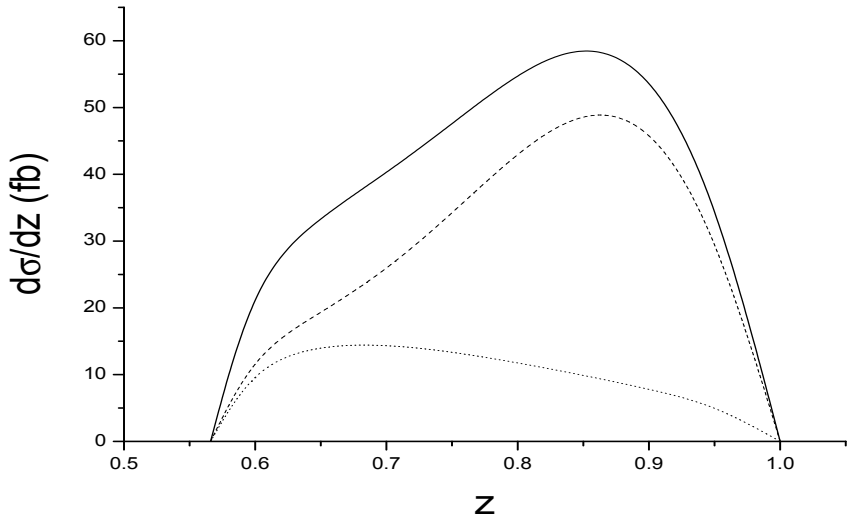

Figure 9: Contributions to $d\sigma(e^+e^- \to \chi_{c1}c\bar{c})/dz$ from color-singlet (dashed line), color-octet (dotted line) and the sum of color-singlet and color-octet (solid line) contributions plotted against z.